Geochemical Perspectives Letters

Continental crust had fully emerged by the end of the Paleoproterozoic

D. Mineart[1], S. Duncanson[1], W. Nachlas[2], B.W. Johnson[1*]

OPEN ACCESS
https://doi.org/10.7185/geochemlet.2551

Abstract

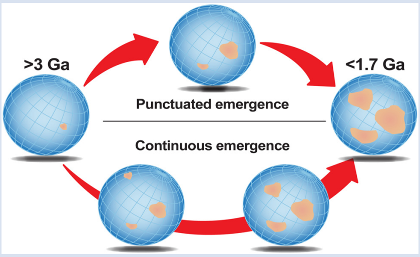

Earth has bimodal hypsometry, with emergent, subaerial continents and submerged oceanic crust. The tempo and history of emergence is imprecisely understood. We estimate the oxygen isotope composition of seawater ($\delta^{18}O_{SW}$) *via* tracer mass balance inversion of sections of hydrothermally altered ocean crust as a proxy for emergent crust. Using data from Sturgeon Lake, Canada (~2735 Ma) and the Pecos Greenstone Belt, USA (~1720 Ma), we find $\delta^{18}O_{SW}$ decreased from about +3 to +4 ‰ to −0.2 ‰, indicating near-modern levels of emergence by ~1720 Ma, with minimal emergence at ~2735 Ma. We employ a steady state $\delta^{18}O_{SW}$ model, driven either by continuous or punctuated continental growth, to interpret our findings. Such reconstructions indicate continental growth and emergence were decoupled until the end of the Archean.

Received 11 November 2024 | Accepted 6 November 2025 | Published 22 December 2025

Introduction

Earth is unique among our planetary neighbours, including the presence of bimodal crust. Dense, oceanic crust underlies large ocean basins today. Buoyant, felsic continental crust is mostly emergent above sea level, giving Earth bimodal hypsometry. Both the presence of substantial felsic crust and its position above sea level exert feedbacks on a planetary scale. Emergent continental crust provides nutrients to the oceans (Large *et al.*, 2018), modulates climate *via* weathering (Walker *et al.*, 1981), and could be an evolutionary driver for life (Zhu *et al.*, 2022).

Determining the tempo and extent of subaerial emergence globally, however, is challenging. While there is a long history of inquiry surrounding the generation of felsic continental crust (Hawkesworth *et al.*, 2024), subaerial emergence is an intertwined, but slightly distinct process. Further, geologic and existing geochemical records of emergence vary widely both in spatial scale and temporal resolution. Limited subaerial emergence, with the Earth resembling a "water world", has been suggested for the early Archean based on water cycle modelling (Korenaga, 2021) and the oxygen isotope value of seawater ($\delta^{18}O_{SW}$)[1] preserved in rocks and minerals (Pope *et al.*, 2012; Bindeman *et al.*, 2018; Johnson and Wing, 2020). Geologic evidence from Archean cratons suggests localised emergence, including ~3.5 Ga angular unconformities (Buick *et al.*, 1995) and ~3.2 Ga river/beach deposits (Heubeck and Lowe, 1994). More widespread emergence at ~2.7 Ga is suggested by large scale passive margin deposits (Bradley, 2008). Mantle thermal modelling, however, suggests that any emergence before the Neoproterozoic was limited to active mountain building regions (Lee *et al.*, 2018). Both crustal and ocean volume contribute to emergence (Korenaga, 2021). To address this uncertainty, we build on previous work using sections of hydrothermally altered ocean crust as a record of $\delta^{18}O_{SW}$ as a proxy for continental emergence (Johnson and Wing, 2020).

$\delta^{18}O_{SW}$ is buffered over million year time scales by water-rock reactions (Gregory, 1991; Muehlenbachs, 1998). Low temperature interactions, both in continental and oceanic crust, move ^{18}O from water to rock, which in turn decreases $\delta^{18}O_{SW}$. High temperature alteration of oceanic crust transfers ^{18}O from rock to water, which would lower $\delta^{18}O_{SW}$. Today, the proportion of low to high temperature alteration in oceanic crust is about equal (Muehlenbachs, 1998), and based on observations of ancient ophiolites and oceanic crust, this proportion was likely similar in the deep past (Holmden and Muehlenbachs, 1993; Johnson and Wing, 2020). Subaerial weathering, in contrast, does not have a high temperature component, so only acts as a sink for ^{18}O. If no crust is emergent, we would expect higher $\delta^{18}O_{SW}$ than if significant crust was emergent. Thus, the proportion of emergent crust, with associated subaerial weathering, should be reflected in variable $\delta^{18}O_{SW}$ over time. We can measure the $\delta^{18}O$ value of sections of hydrothermally altered crust, apply a tracer mass balance inversion approach (Johnson and Wing, 2020), and determine the $\delta^{18}O_{SW}$ of the original seawater as a proxy for crustal emergence.

Current proxies for $\delta^{18}O_{SW}$ come mostly from chemical sediments, including carbonates, chert, phosphates and, since 1.7 Ga, Fe oxides (Isson and Rauzi, 2024). All these records show a secular increase in mineral $\delta^{18}O$ values through time, which

1. Department of the Earth, Atmosphere, and Climate; Iowa State University, Ames, IA, 50011, USA
2. Department of Geoscience, University of Wisconsin Madison; Madison, WI, 53706, USA
* Corresponding author (email: bwj@iastate.edu)

[1] $\delta^{18}O$ (‰) = $[(R_{sample} - R_{std})/R_{std}] \times 1000$ where R_{sample} and R_{std} are the ratio of $^{18}O/^{16}O$ in samples and standards, given in units of per mille (‰). All values presented are relative to Vienna Standard Mean Ocean Water (V-SMOW). The subscript SW refers to seawater values.

has been interpreted to reflect an increase in $\delta^{18}O_{SW}$ from the Proterozoic onwards or a decrease in seawater temperature through time. Estimates of $\delta^{18}O_{SW}$ from the altered ocean crust record suggests a decrease in $\delta^{18}O_{SW}$ from the Paleoarchean to the mid-Proterozoic, or perhaps even as early as the Neoarchean, with little to no change afterwards (Holmden and Muehlenbachs, 1993; Muehlenbachs *et al.*, 2003; Pope *et al.*, 2012; Zakharov and Bindeman, 2019).

In this contribution, we estimated $\delta^{18}O_{SW}$ from two locations: Sturgeon Lake, Canada (~2735 Ma) and the Pecos Greenstone Belt, USA (~1720 Ma). Both sites are associated with volcanogenic massive sulfide (VMS) deposits, which are produced *via* hydrothermal circulation of seawater through oceanic crust. We used bulk rock $\delta^{18}O$ measurements from each site (402 at Sturgeon Lake, 45 at Pecos) along with estimates of alteration temperature (Mg in chlorite for Pecos and O isotopes from Sturgeon) in an inverse model to estimate $\delta^{18}O_{SW}$. We find that $\delta^{18}O_{SW}$ decreased from approximately +3 to +4 ‰ at 2735 Ma to a near-modern value of −0.2 ‰ by ~1720 Ma. We discuss two scenarios that could drive such a shift: continuous or punctuated continental emergence.

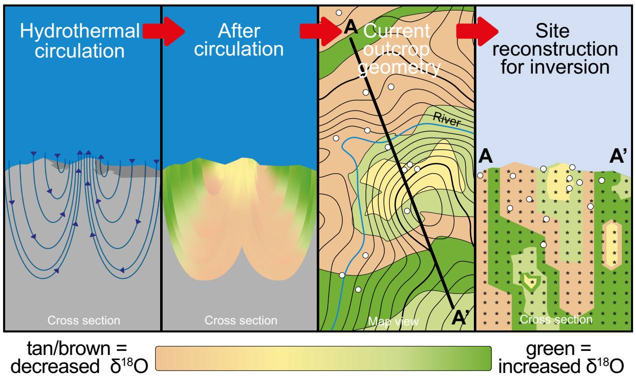

Figure 1 Tracer mass balance inverse approach. When water circulates through rock (leftmost panel), as at a mid-ocean ridge, that circulation causes exchange of O isotopes between water and rock in a well understood, temperature dependent manner (centre left panel). The geometry of patterns of O isotopes produced during circulation may be changed as the rock section ages, undergoes uplift, *etc.* (centre right panel). We then sample across modern outcrops/drill cores, attempt to reconstruct the original geometry, and use this approximation of original isotope and temperature patterns as the basis for inversion (rightmost panel).

Estimating $\delta^{18}O_{SW}$ *via* Inversion of Hydrothermal Systems

Hydrothermal alteration of oceanic crust is a well understood process (Seyfried and Mottl, 1982). The interaction of water and rock at temperatures ranging from bottom water (>2 °C) to peak temperatures of approximately 350–400 °C in oceanic crust causes mineralogical changes, redistribution of elements, and exchange of oxygen isotopes between water and rock (Muehlenbachs, 1998). At low temperatures and shallow crustal depths, ^{18}O is preferentially transferred from water to rock, while for temperatures above 275–300 °C at deep crustal depths, ^{18}O is transferred from rock to water (Cole *et al.*, 1987). The transformation of whole rock $\delta^{18}O$ from an initial value to an altered value is a function of temperature. Therefore, given independent temperature estimates, we can perform a tracer mass balance inversion calculation to estimate the alteration fluid's initial $\delta^{18}O$ (Johnson and Wing, 2020).

This approach proceeds stepwise. We collect samples from across the hydrothermal cell, targeting downwelling and upwelling zones spanning hydrothermal circulation. Discharge zones are assumed to be structurally beneath VMS deposits, while recharge zones are typically 0.5–1 km along strike away from the VMS deposit (Slack *et al.*, 2009). Then, a ~2 D cross section is constructed of each hydrothermal system by extrapolating between irregularly spaced samples into a regularly spaced grid (Figs. 1, 2). The goal is to approximate the original geometry of the active hydrothermal system, with the contours capturing the full horizontal and vertical distribution of the sample set. We contour both whole rock $\delta^{18}O$ and alteration temperature. Temperatures of alteration are estimated either by geothermometry (Mg chlorite; Pecos, see Supplementary Information - SI) or

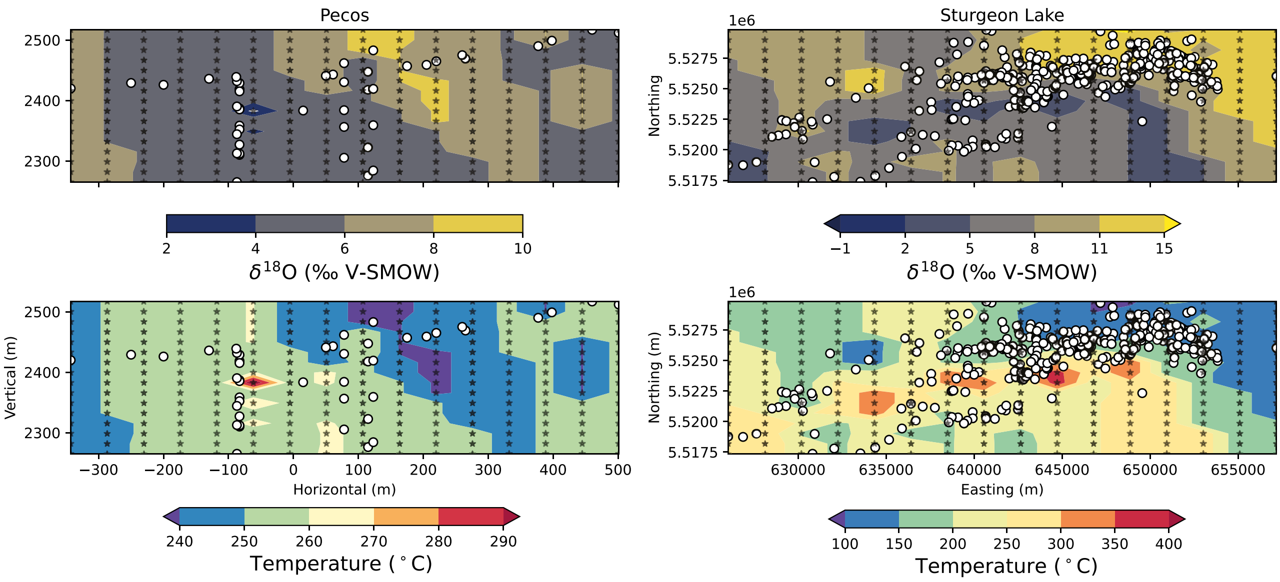

Figure 2 Contoured cross sections of oxygen isotope and alteration temperature for Pecos, NM, USA and Sturgeon Lake, Ontario, Canada. Samples are shown in white circles, grid used in inversion is outlined by the black stars. Cross sections are reconstructed from outcrop and drill core samples to approximate the full hydrothermal cell.

linking distribution of specific mineral phases/mineral pair O isotopes to associated formation temperatures (Sturgeon Lake, see SI).

Then, using $\delta^{18}O$ and temperature inputs, we apply standard linear regression inversion techniques, applying total fluid and oxygen mass balance, to estimate the total fluid required to produce alteration. We use the estimate of total fluid to calculate a fluid/rock ratio (F/R) for the hydrothermal system (see Johnson and Wing, 2020). Key inputs into the inversion include temperature of alteration and initial rock $\delta^{18}O$ ($\delta^{18}O_i$). Initial rock $\delta^{18}O$ value is based either on geologic setting (*e.g.*, mantle derived melts are ∼5.5 ‰) or on analyses of the least altered samples, determined petrographically. Using the estimate of fluid/rock (F/R) ratio from the inversion, we calculate the fluid's initial $\delta^{18}O$ value (δF_i):

$$\delta F_i = \frac{(\delta R_f - \delta R_i)}{F/R} + \delta R_f + \Delta_{R-F}$$

where δR_f and δR_i are the final and initial rock $\delta^{18}O$ values averaged over the cross section. Δ_{R-F} is the average temperature of alteration (Taylor, 1977). This approach was tuned and validated by Johnson and Wing (2020) on Cenozoic sites of known seawater and forward models. We run the inversion the same number of times as there are samples, removing a random sample each time ("leave-one-out") to estimate uncertainty. While we assume isotopic equilibrium, during original method development we also inverted model results that assumed kinetic equilibrium (Johnson and Wing, 2020). In both equilibrium and kinetic cases, the inversion reproduced incoming fluid $\delta^{18}O$. This approach is purely retrospective. It estimates total fluid required for alteration based on the average conditions over the lifetime of the hydrothermal cell.

Sample Sites and Results

Sturgeon Lake. The Sturgeon Lake caldera, ∼2735 Ma, is located in the Sturgeon Lake greenstone belt, a central part of the Wabigoon sub-province in the Archean Superior Province (Fig. S-1; SI). Caldera rocks are primarily felsic, quartz-rich pyroclastic flows with associated VMS deposits. Although the area underwent greenschist-lower amphibolite facies metamorphism, oxygen isotope values retain primary information related to initial hydrothermal alteration (Holk *et al.*, 2008). Isotope contours define the direction of fluid flow during hydrothermal alteration.

We use oxygen isotope data and temperature estimates centred on the Biedelman Bay intrusive complex (Holk *et al.*, 2008). The $\delta^{18}O_i$ at Sturgeon Lake has been estimated between 6–8 ‰, based on analyses of $\delta^{18}O$ in zircons (SI). Whole rock $\delta^{18}O$ values range from 1.2 to 17.9 ‰, with a precision of 0.2 ‰. Temperatures of alteration were estimated using mineral pair fractionations with modelled bulk rock for basalt and rhyolite (Holk *et al.*, 2008). This approach produces temperature estimates that are either low (130–240 °C) or high (175–300 °C), depending on model assumptions.

To account for uncertainty in temperature and initial rock $\delta^{18}O$, we performed the tracer mass balance inversion in four iterations: low (6 ‰) and high (8 ‰) $\delta^{18}O_i$ with either low or high alteration temperature estimates. In each iteration, we still perform "leave-one-out", running the inversion the same number of times as there are samples and removing a random sample each time. We then took the mean and standard deviation from all four iterations, and suggest that seawater $\delta^{18}O$ was and 3.8 ± 0.4 ‰ (1σ) (Fig. 2).

Pecos. The Pecos greenstone belt occupies the southern end of 1.8–1.7 Ga Precambrian supracrustal rocks that extend into Colorado and Wyoming, USA (Slack *et al.*, 2009). The greenstone belt, comprised of bimodal metavolcanics and metasedimentary rocks regionally metamorphosed to greenschist-lower amphibolite facies (Slack *et al.*, 2009), occupies a ∼650 km^2 area northeast of Santa Fe and is bounded in the west by the north-northeast running Picuris-Pecos fault.

We focused on a sample site near the Pecos mine that preserves strong evidence of hydrothermal activity. The area, Willow Creek, comprises a bimodal suite of volcanic rocks (80 % basalt–20 % rhyolite) that likely represent the remnant of a back arc basin or evolved island arc emplaced at ∼1.72 Ga (Slack *et al.*, 2009). Syn-volcanic hydrothermal circulation produced VMS deposits, including at the Pecos mine site. We collected a series of outcrop and drill core samples from the New Mexico Geological Survey for oxygen isotope analyses and chlorite geothermometry (Fig. S-1, SI).

Whole rock $\delta^{18}O$ values were measured using laser fluorination at the Center for Stable Isotopes at the University of New Mexico (Sharp, 1990). Measured whole rock oxygen isotope values range from 2.2 to 9.3 ‰, with a precision of ±0.6 ‰ based on repeat analyses of an olivine standard (SCO; SI). We assumed initial rock $\delta^{18}O$ to be 7.1 ‰, which was the measured value of the least altered sample, determined petrographically. Alteration temperatures were determined for a subset of samples using Mg in chlorite geothermometry (Jowett, 2021), using the Electron Microprobe facility at the University of Wisconsin Madison (SI). Temperatures determined using chlorite thermometry ranged from 350–375 °C, with uncertainty of ±20 °C (1σ). As with Sturgeon Lake, we assigned an estimated alteration temperature for each sample based on observed correlation between $\delta^{18}O$ and Mg in chlorite temperatures (SI).

To account for analytical uncertainty in these samples, we performed the tracer mass balance inversion (with "leave-one-out") for five iterations, all assuming $\delta^{18}O_i = 7.1$ ‰: (1) nominal, with mean values for all sample $\delta^{18}O$ and Mg chlorite temperatures, (2) upper estimate (*i.e.* mean plus uncertainty) sample $\delta^{18}O$, and Mg chlorite temperatures, (3) lower sample (*i.e.* mean minus uncertainty) $\delta^{18}O$ and Mg chlorite temperatures, (4) upper $\delta^{18}O$ and lower Mg chlorite temperatures, and (5) lower $\delta^{18}O$ and upper Mg chlorite temperatures. As with the previous section, we report the mean seawater $\delta^{18}O$ from these five iterations, which we find to be 0.3 ± 1.2 ‰ (1σ) (Fig. 2). The uncertainty at Pecos is higher than at Sturgeon Lake primarily due to lower sample numbers.

Near-Modern Emergence by the Paleoproterozoic

Previous work estimated $\delta^{18}O_{SW}$ at ∼3240 Ma to be 3.3 ± 0.1 ‰ (Johnson and Wing, 2020). We find a similar value at Sturgeon Lake, with $\delta^{18}O_{SW}$ of 3.8 ± 0.4 ‰ at ∼2735 Ma, and a near-modern value at Pecos (∼1720 Ma) of 0.3 ± 1.2 ‰ (Fig. 3). This decrease can be explained by the emergence of continental crust with associated weathering and sequestration of ^{18}O (Johnson and Wing, 2020). The timing of widespread emergence suggested by our results is consistent with estimates from O isotope composition of shales (Bindeman *et al.*, 2018), the presence of large passive margins (Bradley, 2008), and calculation of heat production in Archean lithosphere (Reimink and Smye, 2024).

To investigate how emergence could cause changes in $\delta^{18}O_{SW}$, we calculated two potential evolutionary curves of $\delta^{18}O_{SW}$ based on a steady state model (Muehlenbachs, 1998).

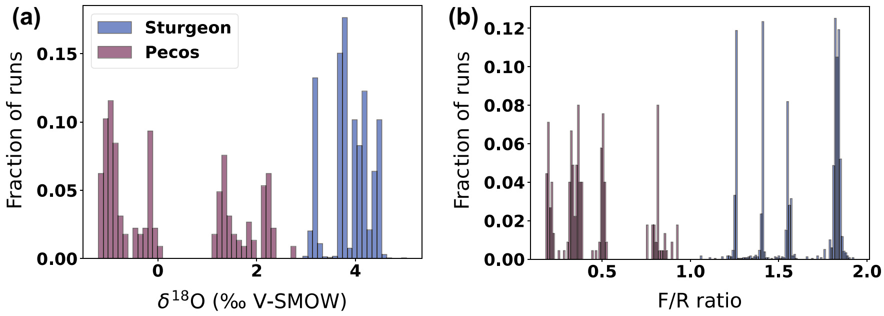

Figure 3 Histograms of 'leave-one-out' inversions showing both estimated initial **(a)** fluid $\delta^{18}O$, and **(b)** fluid-rock ratio. Inversions are performed the same number of times as there are samples at a given location, removing a random sample each time to constrain uncertainty, for a series of iterations at each site spanning temperature and/or starting rock $\delta^{18}O$ values.

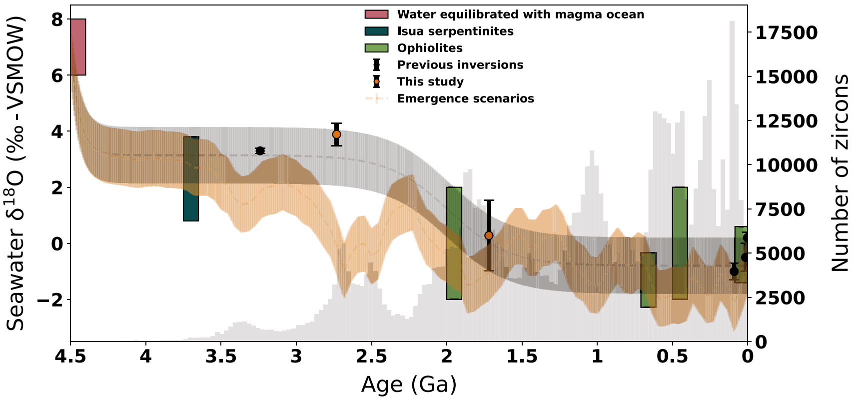

Figure 4 Estimates of seawater $\delta^{18}O$ from altered ocean crust (green rectangles; Gregory, 1991; Holmden and Muehlenbachs, 1993; Pope *et al.*, 2012) previous (black circles, Johnson and Wing, 2020), and this study's, tracer mass balance inversion estimates (orange circles). Also shown are abundance of detrital zircon ages in 30 Myr time bins (Puetz *et al.*, 2024) and two seawater $\delta^{18}O$ evolution curves (Muehlenbachs, 1998): (1) continuous crustal growth and emergence (gray dashed line), and (2) punctuated curve driven by zircon abundance (orange dashed line). Seawater evolution curves are shown with ±1 ‰ envelopes, equivalent to observed changes in the $\delta^{18}O_{SW}$ during Pleistocene glaciations (Schrag *et al.*, 2002).

This steady state model estimates total water-rock fluxes and associated isotopic fractionations based on the modern Earth, and includes high and low temperature alteration, subaerial weathering, effects during continental growth, and water recycling into and out of the mantle. We used water flux and fractionation values directly from the original manuscript except we increased fractionation during subaerial weathering (12 ‰) to produce a modern, ice free ocean at -1 ‰ (Johnson and Wing, 2020). We assume no change in the proportion of high to low temperature submarine alteration over time (SI).

We then run this steady state model without any continental fluxes initially, then increase them over Earth history. We produce two scenarios of continental emergence (Fig. 4): (1) relatively smooth, continuous growth of continental crust and implied emergence from between 3 to 1 Ga (Reimink *et al.*, 2023; Reimink and Smye, 2024), or (2) a punctuated model with weathering fluxes normalised to the abundance of detrital zircon ages over time (zircon ages from Puetz *et al.*, 2024). We detail our steady state model calculations in the SI. Zircon abundances have been de-trended, assuming 97 % survival rate *per* 30 Myr time bin (Puetz *et al.*, 2024).

Both scenarios (continuous emergence, punctuated) are consistent with relatively high $\delta^{18}O_{SW}$ in the Archean, until about 3 Ga. High $\delta^{18}O_{SW}$ is maintained by limited continental weathering. The $\delta^{18}O_{SW}$ then decreases in both scenarios, although at slightly different times. The continuous model decreases between 3 to 1 Ga, while the punctuated model decreases towards modern $\delta^{18}O_{SW}$ between 3–2.7 Ga, increases to ~2 ‰ between 2.7–2.3 Ga, and then decreased in an oscillatory pattern towards modern values by 0.8 Ga.

If $\delta^{18}O_{SW}$ followed either of these evolutionary pathways, modern values were present by the Mesoproterozoic. Approximately 25–35 % of the modern sedimentary rock volume would be a sufficient sink for ^{18}O to cause ~4 ‰ decrease between the Archean and end of the Proterozoic (Johnson and Wing, 2020). The two scenarios differ in $\delta^{18}O_{SW}$ in the late Archean. Perhaps the first peaks in the detrital zircon record reflect continental crust growth that was not associated with emergence and weathering. That is, continental growth and weathering were not coupled until the end of the Archean and throughout the Proterozoic. While growth is a prerequisite for emergence, they may not necessarily occur at the same time.

Conclusions

We used tracer mass balance inverse modelling of sections of altered ocean crust to estimate $\delta^{18}O_{SW}$ during the Neoarchean through Paleoproterozoic. By analysing data from Sturgeon Lake, Ontario, Canada and Pecos, NM, USA, we estimate that OISW decreased from +3 ‰ to +4 ‰ to ~0 ‰ between 2.7 and 1.72 Ga.

This decrease could be caused by emergence of landforms, with associated weathering and sequestration of ^{18}O into weathered continental crust. We demonstrate, through an $\delta^{18}O_{SW}$ steady state model, that such a mechanism can indeed cause the observed drop in $\delta^{18}O_{SW}$. We present two potential $\delta^{18}O_{SW}$ evolutionary curves, continuous and punctuated. These curves are driven either by steady crustal growth and emergence or growth and emergence that varies, as reflected in the detrital zircon record. These two reconstructions suggest, when compared with tracer mass balance estimates, decoupled continental growth and emergence until the end of the Archean and throughout the Proterozoic. Only after substantial crustal growth has occurred is emergence likely, reflected in the decrease in $\delta^{18}O_{SW}$.

Acknowledgements

We thank Zachary Sharp and the Center for Stable Isotopes at the University of New Mexico for $\delta^{18}O$ analyses and three anonymous reviewers for constructive feedback. We also thank Annabelle Lopez at New Mexico Tech for facilitating drill core sampling and metadata.

Editor: Gavin Foster

Additional Information

Supplementary Information accompanies this letter at https://www.geochemicalperspectivesletters.org/article2551.

Cite this letter as: Mineart, D., Duncanson, S., Nachlas, W., Johnson, B.W. (2025) Continental crust had fully emerged by the end of the Paleoproterozoic. *Geochem. Persp. Let.* 38, 23–28. https://doi.org/10.7185/geochemlet.2551

References

Bindeman, I.N., Zakharov, D.O., Palandri, J., Greber, N.D., Dauphas, N., Retallack, G.J., Hofmann, A., Lackey, J.S., Bekker, A. (2018) Rapid emergence of subaerial landmasses and onset of a modern hydrologic cycle 2.5 billion years ago. *Nature* 557, 545–548. https://doi.org/10.1038/s41586-018-0131-1

Bradley, D.C. (2008) Passive margins through earth history. *Earth-Science Reviews* 91, 1–26. https://doi.org/10.1016/j.earscirev.2008.08.001

Buick, R., Thornett, J.R., McNaughton, N.J., Smith, J.B., Barley, M.E., Savage, M. (1995) Record of emergent continental crust ~3.5 billion years ago in the Pilbara craton of Australia. *Nature* 375, 574–577. https://doi.org/10.1038/375574a0

Cole, D.R., Mottl, M.J., Ohmoto, H. (1987) Isotopic exchange in mineral-fluid systems. II. Oxygen and hydrogen isotopic investigation of the experimental basalt-seawater system. *Geochimica et Cosmochimica Acta* 51, 1523–1538. https://doi.org/10.1016/0016-7037(87)90334-6

Gregory, R. (1991) Oxygen isotope history of seawater revisited: Timescales for boundary event changes in the oxygen isotope composition of seawater. In: Taylor Jr., H.P., O'Neil, J.R., Kaplan, I.R. (Eds.) *Stable Isotope Geochemistry: A Tribute to Samuel Epstein*. Geochemical Society, San Antonio, 65–76. https://geochemsoc.org/application/files/6917/5333/2164/SP-3_065-076_Gregory.pdf

Hawkesworth, C., Cawood, P.A., Dhuime, B., Kemp, T. (2024) Tectonic processes and the evolution of the continental crust. *Journal of the Geological Society* 181, jgs2024-027. https://doi.org/10.1144/jgs2024-027

Heubeck, C., Lowe, D.R. (1994) Depositional and tectonic setting of the Archean Moodies Group, Barberton Greenstone Belt, South Africa. *Precambrian Research* 68, 257–290. https://doi.org/10.1016/0301-9268(94)90033-7

Holk, G.J., Taylor, B.E., Galley, A.G. (2008) Oxygen isotope mapping of the Archean Sturgeon Lake caldera complex and VMS-related hydrothermal system, Northwestern Ontario, Canada. *Mineralium Deposita* 43, 623–640. https://doi.org/10.1007/s00126-008-0185-3

Holmden, C., Muehlenbachs, K. (1993) The $^{18}O/^{16}O$ Ratio of 2-Billion-Year-Old Seawater Inferred from Ancient Oceanic Crust. *Science* 259, 1733–1736. https://doi.org/10.1126/science.259.5102.1733

Isson, T., Rauzi, S. (2024) Oxygen isotope ensemble reveals Earth's seawater, temperature, and carbon cycle history. *Science* 383, 666–670. https://doi.org/10.1126/science.adg1366

Johnson, B.W., Wing, B.A. (2020) Limited Archaean continental emergence reflected in an early Archaean ^{18}O-enriched ocean. *Nature Geoscience* 13, 243–248. https://doi.org/10.1038/s41561-020-0538-9

Jowett, E.C. (2021) Fitting Iron and Magnesium into the Hydrothermal Chlorite Geothermometer. *SSRN Electronic Journal*. https://doi.org/10.2139/ssrn.3863523

Korenaga, J. (2021) Was There Land on the Early Earth? *Life* 11, 1142. https://doi.org/10.3390/life11111142

Large, R.R., Mukherjee, I., Zhukova, I., Corkrey, R., Stepanov, A., Danyushevsky, L.V. (2018) Role of upper-most crustal composition in the evolution of the Precambrian ocean–atmosphere system. *Earth and Planetary Science Letters* 487, 44–53. https://doi.org/10.1016/j.epsl.2018.01.019

Lee, C.-T.A., Caves, J., Jiang, H., Cao, W., Lenardic, A., McKenzie, N.R., Shorttle, O., Yin, Q.-z., Dyer, B. (2018) Deep mantle roots and continental emergence: implications for whole-Earth elemental cycling, long-term climate, and the Cambrian explosion. *International Geology Review* 60, 431–448. https://doi.org/10.1080/00206814.2017.1340853

Muehlenbachs, K. (1998) The oxygen isotopic composition of the oceans, sediments and the seafloor. *Chemical Geology* 145, 263–273. https://doi.org/10.1016/S0009-2541(97)00147-2

Muehlenbachs, K., Furnes, H., Fonneland, H.C., Hellevang, B. (2003) Ophiolites as faithful records of the oxygen isotope ratio of ancient seawater: the Solund-Stavfjord Ophiolite Complex as a Late Ordovician example. In: Dilek, Y., Robinson, P.T. (Eds.) *Ophiolites in Earth History*. Geological Society, London, 401–414. https://doi.org/10.1144/GSL.SP.2003.218.01.20

Pope, E.C., Bird, D.K., Rosing, M.T. (2012) Isotope composition and volume of Earth's early oceans. *Proceedings of the National Academy of Sciences* 109, 4371–4376. https://doi.org/10.1073/pnas.1115705109

Puetz, S.J., Spencer, C.J., Condie, K.C., Roberts, N.M.W. (2024) Enhanced U-Pb detrital zircon, Lu-Hf zircon, $\delta^{18}O$ zircon, and Sm-Nd whole rock global databases. *Scientific Data* 11, 56. https://doi.org/10.1038/s41597-023-02902-9

Reimink, J.R., Smye, A.J. (2024) Subaerial weathering drove stabilization of continents. *Nature* 629, 609–615. https://doi.org/10.1038/s41586-024-07307-1

Reimink, J.R., Davies, J.H.F.L., Moyen, J.-F., Pearson, D.G. (2023) A whole-lithosphere view of continental growth. *Geochemical Perspectives Letters* 26, 45–49. https://doi.org/10.7185/geochemlet.2324

Schrag, D.P., Adkins, J.F., McIntyre, K., Alexander, J.L., Hodell, D.A., Charles, C.D., McManus, J.F. (2002) The oxygen isotopic composition of seawater during the Last Glacial Maximum. *Quaternary Science Reviews* 21, 331–342. https://doi.org/10.1016/S0277-3791(01)00110-X

Seyfried Jr., W.E., Mottl, M.J. (1982) Hydrothermal alteration of basalt by seawater under seawater-dominated conditions. *Geochimica et Cosmochimica Acta* 46, 985–1002. https://doi.org/10.1016/0016-7037(82)90054-0

Sharp, Z.D. (1990) A laser-based microanalytical method for the *in situ* determination of oxygen isotope ratios of silicates and oxides. *Geochimica et Cosmochimica Acta* 54, 1353–1357. https://doi.org/10.1016/0016-7037(90)90160-M

Slack, J.F., Grenne, T., Bekker, A. (2009) Seafloor-hydrothermal Si-Fe-Mn exhalites in the Pecos greenstone belt, New Mexico, and the redox state of ca. 1720 Ma deep seawater. *Geosphere* 5, 302–314. https://doi.org/10.1130/GES00220.1

Taylor Jr., H.P. (1977) Water/rock interactions and the origin of H_2O in granitic batholiths: Thirtieth William Smith lecture. *Journal of the Geological Society* 133, 509–558. https://doi.org/10.1144/gsjgs.133.6.0509

Walker, J.C.G., Hays, P.B., Kasting, J.F. (1981) A negative feedback mechanism for the long-term stabilization of Earth's surface temperature. *Journal of Geophysical Research: Oceans* 86, 9776–9782. https://doi.org/10.1029/JC086iC10p09776

Zakharov, D.O., Bindeman, I.N. (2019) Triple oxygen and hydrogen isotopic study of hydrothermally altered rocks from the 2.43–2.41 Ga Vetreny belt, Russia: An insight into the early Paleoproterozoic seawater. *Geochimica et Cosmochimica Acta* 248, 185–209. https://doi.org/10.1016/j.gca.2019.01.014

Zhu, Z., Campbell, I.H., Allen, C.M., Brocks, J.J., Chen, B. (2022) The temporal distribution of Earth's supermountains and their potential link to the rise of atmospheric oxygen and biological evolution. *Earth and Planetary Science Letters* 580, 117391. https://doi.org/10.1016/j.epsl.2022.117391